Quantitative, three-dimensional diagnostics of multiphase drop fragmentation via digital in-line holography

Jian Gao,[1] Daniel R. Guildenbecher,[2] Phillip L. Reu,[2] Varun Kulkarni,[1] Paul E. Sojka,[1] and Jun Chen[1,*]

[1]*School of Mechanical Engineering, Purdue University, West Lafayette, Indiana 47907, USA*

[2]*Sandia National Laboratories, Albuquerque, New Mexico 87185, USA*

**Corresponding author: junchen@purdue.edu*

Received March 26, 2013; revised May 1, 2013; accepted May 2, 2013;
posted May 2, 2013 (Doc. ID 187246); published May 24, 2013

Quantitative application of digital in-line holography (DIH) to characterize multiphase fragmentation is demonstrated. DIH is applied to record sequential holograms of the breakup of an ethanol droplet in an aerodynamic flow field. Various stages of the breakup process are recorded, including deformation, bag growth, bag breakup, and rim breakup. A recently proposed hybrid method is applied to extract the three-dimensional (3D) location and size of secondary droplets as well as the 3D morphology of the rim. Particle matching between sequential frames is used to determine the velocity. Coincidence with the results obtained from phase Doppler anemometry measurement demonstrates the accuracy of measurement by DIH and the hybrid method.

OCIS codes: (090.1995) Digital holography; (120.0120) Instrumentation, measurement, and metrology; (100.6890) Three-dimensional image processing.

http://dx.doi.org/10.1364/OL.38.001893

Many multiphase flow processes, with applications to the natural and applied sciences, involve the formation and fragmentation of liquid drops or gaseous bubbles. Development and validation of first-principle models require experimental measurements of breakup processes, which often include complex three-dimensional (3D) morphology, the formation of highly nonspherical ligaments, and rapid temporal variations. For example, the breakup of a single drop subjected to aerodynamic forces is of relevance to pharmaceutical/medical sprays, fuel injection, consumer/food processing applications, and surface painting/coating. Theoretical and analytical models describing this process are subject to considerable criticism. Previous breakup models based on boundary layer effects may be incorrect [1], and current debate focuses on the relative importance of Kelvin–Helmholtz and Rayleigh–Taylor instabilities [2]. Contributing to the confusion is the lack of 3D, time-resolved experimental characterization of the dynamic process with sufficient spatial resolution to interrogate both large (parent drop, rim, or core) and small scale (children drop) structures.

Common diagnostic techniques for multiphase flows, such as phase Doppler anemometry (PDA) and two-dimensional (2D) imaging, are unable to resolve the full 3D spatial distribution of particle sizes and velocities without significant experimental repetition, and, in the case of PDA, are limited to spherical particles. Digital holography, on the other hand, promises unique access to 3D information [3] and refractive indices [4]. Previously, digital in-line holography (DIH) has been combined with tomographic techniques to extract the morphology of drops of simple shapes [5]. Furthermore, submicrometer accuracy has been reported for the size and 3D position of particles [6,7] when applications are limited to dilute fields of spherical particles. Finally, DIH has been applied to a somewhat denser droplet field generated by a nozzle [8]; however, the measurement accuracy was only partially validated by comparing the mean diameter and velocity with PDA measurements. Consequently, accurate methods to characterize 3D, multiphase flows have yet to be proven, especially when the particle field consists of denser particles of nonspherical shapes and intermediate fragments of complex morphologies.

In the present study, DIH is applied to characterize aerodynamic fragmentation of a liquid drop. Figure 1 shows the experimental configuration for double-exposure DIH. The origin of the coordinate system is set at the center of the circular outlet of an air nozzle, as also shown in Fig. 2. An ethanol drop is produced by a dispensing tip placed at ($x = 10$ mm, $y = -128$ mm, $z = 0$ mm). The drop leaves the dispensing tip with near-zero velocity and accelerates by gravity into the air jet. A Coriolis mass-flow sensor is used to monitor the total flow rate in the nozzle such that the air-jet velocities can be estimated from previous measurements [9]. For the results reported here, the total air mass-flow rate is 0.35 ± 0.01 kg/min. The Weber number, $\mathrm{We} = \rho_a u_0^2 d_0/\sigma$, which describes the ratio of disruptive aerodynamic drag forces to restorative surface tension forces, is about 11, which corresponds to the bag breakup regime [1]. Here, ρ_a is the density of the ambient air, $u_0 \approx 9$ m/s is the initial relative velocity between the air and the drop, $d_0 \approx 2.58$ mm is the initial diameter of the drop, and σ is the surface tension.

The beam from a double-pulsed Nd:YAG laser (532 nm, 5 ns pulsewidth) is spatially filtered, expanded, and collimated before passing through the region of drop breakup, perpendicular to the main flow direction. Pulse

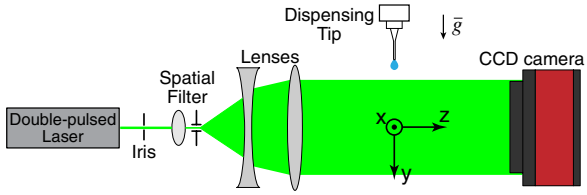

Fig. 1. Double-exposure DIH configuration for characterizing drop fragmentation.

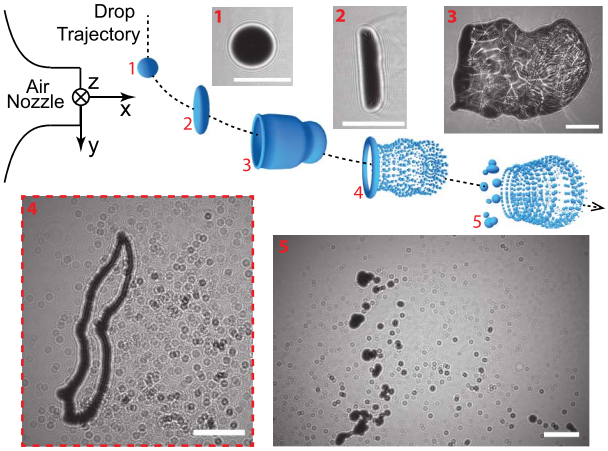

Fig. 2. Illustration of the bag breakup process and the corresponding holograms. The scale bar is 4 mm.

energy is adjusted by altering the time delay between the flashlamp and Q switch of the laser. To synchronize the breakup event with the DIH system, a He–Ne laser and a photodetector (not shown in Fig. 1) are used to generate a trigger signal when the He–Ne beam path is blocked by the falling drop. A pair of in-line holograms is recorded by an interline transfer CCD camera (4008×2672 pixels, 9×9 μm^2/pixel) operating in double-exposure mode, with the delay between holograms determined by the temporal separation of the first and second laser pulses, $\Delta t = 62$ μs.

Figure 2 shows holograms recorded at different times after the drop enters the air jet. Morphological development consistent with bag-type breakup [1] is observed. Initially the drop deforms into a disk-like shape and then to a thin hollow bag attached to a thicker toroidal rim. After that the bag breaks up into a large number of small drops, followed by the disintegration of the rim. Note, illustrating holograms are cropped from full-size holograms corresponding to each breakup stage.

The angular spectrum method [10] is used to reconstruct the complex amplitude E_r from the hologram:

$$E_r(k,l,z_r) = \mathcal{F}^{-1}\left\{\mathcal{F}\{h(m,n)\} \times \exp\left(jkz_r\sqrt{1-\left(\frac{\lambda m}{M\Delta\xi}\right)^2-\left(\frac{\lambda n}{N\Delta\eta}\right)^2}\right)\right\}, \quad (1)$$

where z_r is the reconstruction distance, $h(m,n)$ is the recorded hologram, k is the wave number, λ is the wavelength, M and N are the number of pixels in the horizontal and vertical directions, and $\Delta\xi$ and $\Delta\eta$ are the dimensions of an individual pixel. $\mathcal{F}$ and $\mathcal{F}^{-1}$ denote the fast Fourier transform and inverse fast Fourier transform, respectively. A recently developed hybrid method [11] is used to extract the droplet information. This method features automatic selection of optimum segmentation thresholds for each particle and validated capability to detect nonspherical particles. Here, the diameter of a nonspherical particle is determined as that of a spherical particle with an equivalent cross-sectional area. The minimum detectable diameter is set to 30 μm (~3 pixels). The match probability method [12] is applied to determine 3D displacements ($\Delta\vec{x}$) of detected particles in two consecutive holograms. Accordingly, the 3D particle velocity is measured by $\Delta\vec{u} = \Delta\vec{x}/\Delta t$. Finally, the 3D geometry of the rim is determined assuming the rim is composed of differential tube segments with circular cross sections. Edge pixels of each segment are identified first (using the maximum Tenengrad map defined in [11]), and each edge pixel is associated with a 3D coordinate (according to the depth map). Accordingly, the diameter, center location, and orientation of each segment are determined from the edge pixels. The connection of differential segments together produces the rim.

Using the methods described, the hologram pair highlighted in Fig. 2 is processed, and the measured rim geometry and drop size and velocity are shown in Fig. 3. The total volume of all detected secondary drops is 10.2% that of the initial drop, and the measured volume of the rim corresponds to 92.0% of the initial volume, indicating a 2.2% discrepancy in measured rim and/or drop volume. These results indicate that previous estimations for the volume ratio of the rim (56%) [13] may not be valid for all conditions and further investigations are warranted.

The dominant velocity component is in the $+x$ direction due to the aerodynamic drag. Disintegration of the bag also casts the droplets outward radially in the y–z plane. To illustrate this, Fig. 4 shows the same results as in Fig. 3 but viewed from the $+x$ direction. The mean and standard deviations of the relative velocity components in the four regions, which are divided according to the geometric center of the rim, are also shown. An approximate symmetry of mean velocities can be seen with respect to the rim center. Physically, one expects the standard deviation of $V_{y,\mathrm{rel}}$ and $V_{z,\mathrm{rel}}$ to be similar, while the higher measured value for the z component is indicative of increased measurement uncertainty in this direction, as is expected in the reconstructed depth direction in DIH [6–8].

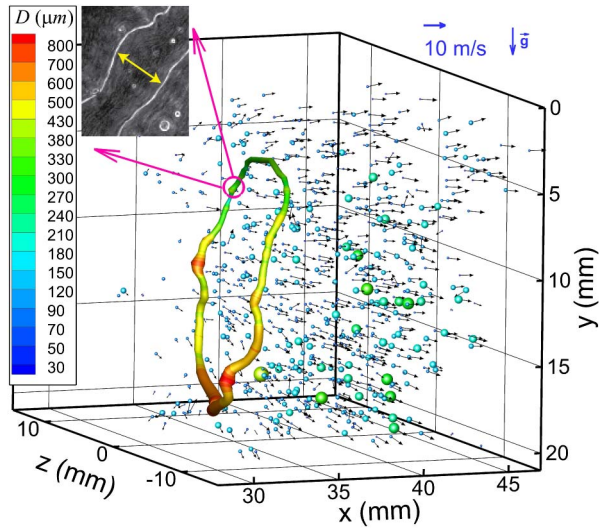

Fig. 3. 3D representation of the measured morphology of the rim, drop spatial distribution, size, and velocity. Inset: cropped maximum Tenengrad map. D: diameter.

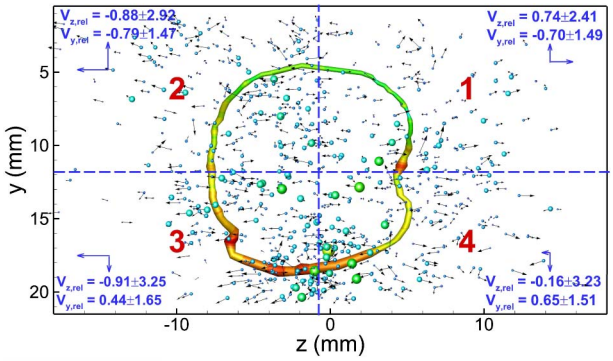

Fig. 4. Droplet field in Fig. 3 viewed from the $+x$ direction. $V_{y,\mathrm{rel}}$ and $V_{z,\mathrm{rel}}$ are the mean droplet velocities in each quadrant. Note that V_{rel} is the relative velocity with respect to the rim, i.e., $V_{\mathrm{rel}} = V_{\mathrm{drop}} - V_{\mathrm{rim}}$; different vector length scales are used for the individual particle velocities (black) and mean velocity (blue). Unit: m/s.

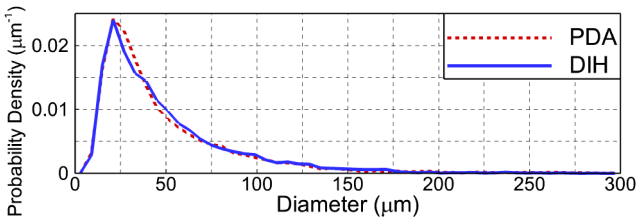

Fig. 5. Size distribution measured by PDA and DIH.

To further demonstrate the accuracy of the measurements, results from DIH are compared with those from PDA measurements under identical experimental conditions. The PDA system (Dantec Dynamics) measures drop size and 2D velocity (in the x–y plane) at a downstream point ($x = 150$ mm, $y = 17$ mm, $z = 0$ mm), where the initial drop has fully broken into secondary drops of spherical shapes. To overcome the lower limit of the detectable diameter (30 μm), a lens is placed between the object and the CCD to introduce a magnification in the DIH system. Calibration is performed to determine the precise distance between the camera and the lens, and a magnification of 3.5 is achieved. 11508 drops are measured by the PDA, and 4105 are detected from 18 holograms using DIH. The DIH measurement volume is located where the bag has broken into droplets, yet the rim remains intact. Therefore, DIH measures only the small droplets produced by breakup of the bag, while the downstream PDA measurement may include larger drops formed from breakup of the rim. Nevertheless, as shown in Fig. 5, agreement between DIH and PDA for the size distribution is quite good. This is likely because the number of drops produced from breakup of the bag is significantly greater than the number produced from breakup of the rim. Furthermore, Table 1 compares the measured mean droplet diameters and velocities, where the definitions of the mean diameters can be found in [1]. The discrepancies in mean velocities can be attributed to differences in measurement location, noting that drops measured by the downstream PDA have been further accelerated by aerodynamic drag.

Table 1. Comparison of Measured Mean Diameters (μm) and Velocities (m/s)

	D_{10}	D_{30}	D_{32}	V_x	V_y
PDA	48.97	78.73	123.87	7.65	0.44
DIH	49.42	76.45	115.96	4.54	0.66

Here, it is shown that digital holography, along with recently developed particle detection algorithms, forms an excellent tool for the study of multiphase fragmentation processes with unique features, such as volumetric detection, the capability to measure 3D velocities, and applicability to nonspherical particles without knowledge of the refractive index. The accuracy of the measured particle sizes is verified with downstream PDA results. Finally, the potential of DIH to extract highly nonspherical 3D morphologies is also demonstrated.

This work is supported by Sandia National Laboratories, a multiprogram laboratory operated by Sandia Corporation, a Lockheed Martin Company, for the United States Department of Energy's National Nuclear Security Administration under contract no. DE-AC04-94AL85000.

References

1. D. Guildenbecher, C. López-Rivera, and P. Sojka, Exp. Fluids **46**, 371 (2009).
2. T. Theofanous, Annu. Rev. Fluid Mech. **43**, 661 (2011).
3. U. Schnars and W. Jüptner, Appl. Opt. **33**, 179 (1994).
4. K. Yassien, M. Agour, C. von Kopylow, and H. El-Dessouky, Opt. Lasers Eng. **48**, 555 (2010).
5. G. Nehmetallah and P. Banerjee, Proc. SPIE **7851**, 78510I (2010).
6. F. Soulez, L. Denis, C. Fournier, É. Thiébaut, and C. Goepfert, J. Opt. Soc. Am. A **24**, 1164 (2007).
7. J. Lu, R. Shaw, and W. Yang, Opt. Express **20**, 12666 (2012).
8. Y. Yang and B. Kang, Opt. Lasers Eng. **49**, 1254 (2011).
9. A. Flock, D. Guildenbecher, J. Chen, P. Sojka, and H. Bauer, Int. J. Multiphase Flow **47**, 37 (2012).
10. J. Goodman, *Introduction to Fourier Optics* (McGraw-Hill, 1996), pp. 55–61.
11. D. Guildenbecher, J. Gao, P. Reu, and J. Chen, "Digital holography simulations and experiments to quantify the accuracy of 3D particle location and 2D sizing using a proposed hybrid method," Appl. Opt. (to be published).
12. S. Baek and S. Lee, Exp. Fluids **22**, 23 (1996).
13. W. Chou and G. Faeth, Int. J. Multiphase Flow **24**, 889 (1998).